Analysis of the Weak Interactions of ADP-Unc104 and ADP-Kinesin with Microtubules and their Inhibition by MAP2c

Jawdat Al-Bassam, Benoit Roger, Shelley Halpain, and Ronald A. Milligan*

Department of Cell Biology, The Scripps Research Institute, La Jolla, California 92037

Microtubule based motors like conventional kinesin (Kinesin-1) and Unc104 (Kinesin-3), and classical microtubule associated proteins (MAPs), including MAP2, are intimately involved in neurite formation and organelle transport. The processive motility of both these kinesins involves weak microtubule interactions in the ADP-bound states. Using cosedimentation assays, we have investigated these weak interactions and characterized their inhibition by MAP2c. We show that Unc104 binds microtubules with five-fold weaker affinity and two-fold higher stoichiometry compared with conventional kinesin. Unc104 and conventional kinesin binding affinities are primarily dependent on positively charged residues in the Unc104 K-loop and conventional kinesin neck coiled-coil and removal of these residues affects Unc104 and conventional kinesin differently. We observed that MAP2c acts primarily as a competitive inhibitor of Unc104 but a mixed inhibitor of conventional kinesin. Our data suggest a specific model in which MAP2c differentially interferes with each kinesin motor by inhibiting its weak attachment to the tubulin C-termini. This is reminiscent of the defects we have observed in Unc104 and kinesin mutants in which the positively charged residues in K-loop and neck coiled-coil domains were removed. Cell Motil. Cytoskeleton 64: 377–389, 2007.   © 2007 Wiley-Liss, Inc.

INTRODUCTION

Neuronal axons and dendrites require the transport of organelles and macromolecules from the cell body toward their tips during and after development [Goldstein, 2001; Hirokawa and Takemura, 2005]. A variety of membranous organelles are transported along microtubules by motor proteins from the kinesin superfamily [Brown, 2003]. Unc104/KIF1 kinesins (kinesin-3 class; termed Unc104 herein) and conventional kinesins (kinesin-1 class; termed kinesin herein) represent two unique classes of plus-end directed motors that are extensively utilized in neurons. Kinesin generally transports neurofilaments, vesicles containing amyloid precursor protein (APP), and glutamate receptors [Goldstein, 2001; Setou et al., 2002]. In contrast, Unc104/KIF1 kinesins transport synaptic vesicle precursors and mitochondria [Hall and Hedgecock, 1991; Nangaku et al., 1994]. Unc104 moves along microtubules two to three times faster than kinesin both in vitro and in vivo

[Pierce et al., 1999; Zhou et al., 2001]. Although Unc104 is monomeric in solution, it is believed to dimerize when clustered on vesicles, allowing it to walk processively along microtubules by a hand-over-hand mechanism similar to kinesin [Romberg et al., 1998; Tomishige

*Correspondence to: Ronald A. Milligan, Dept Cell Biology CB-227, The Scripps Research Institute, La Jolla, CA 92037, USA.
E-mail: milligan@scripps.edu

Jawdat Al-Bassam's present address is Department of Biochemistry and Molecular Pharmacology, Harvard Medical School, Boston, MA 02115, USA.

et al., 2002]. In this model, one motor domain of the ADP-containing dimer initially interacts weakly with a binding site on the microtubule. This initial interaction in the motility cycle is the one we have focused on in this work. ADP is quickly released and ATP binds, forming a strongly bound state and eliciting a conformational change in the attached head that positions the partner head near the next binding site where it can initiate its own cycle of binding and hydrolysis. Alternating catalysis by the two heads of the dimer, coupled with conformational changes, results in walking of the dimer along consecutive sites on the protofilament surface [reviewed in Vale and Milligan, 2000].

The kinesin motor binds over the β-tubulin C-terminus, whereas the α tubulin C-terminus lies between motor binding sites [Hoenger et al., 1998; Kikkawa et al., 2000]. Mutagenesis analysis suggests that the N-terminal part of the kinesin neck coiled coil interacts with the disordered α tubulin C-termini [Thorn et al., 2000]. In Unc104, the K-loop, a class-specific insert in L-12 that is not found in conventional kinesins, binds the β-tubulin C-termini [Kikkawa et al., 2001; Al-Bassam et al., 2003].

Microtubules are dynamic polymers that undergo phases of assembly and disassembly [Mitchison and Kirschner, 1984; Desai and Mitchison, 1997]. In neurons, these dynamic properties are regulated by microtubule associated proteins (MAPs) that stabilize or destabilize microtubules [Dehmelt and Halpain, 2004; Gordon-Weeks, 2004]. MAP2 and tau are well-characterized neuronal MAPs that share high homology in their microtubule binding domain, which consists of multiple 31-residue repeats [Dehmelt and Halpain, 2005]. MAP2 and tau bind along microtubules and increase microtubule stability by decreasing the frequency of catastrophes and increasing rescues [Kowalski and Williams, 1993; Gamblin et al., 1996]. MAP2 and tau binding is largely dependent on the presence of the disordered tubulin C-termini, as their removal by subtilisin proteolysis abolishes most of the MAP binding affinity to microtubules [Serrano et al., 1984, 1985]. On binding to microtubules, MAP2 and tau adopt an ordered conformation along the outer ridges of the microtubule protofilaments, where the tubulin C-termini emanate from the microtubule surface [Al-Bassam et al., 2002]

MAP2 or tau binding to microtubules inhibits kinesin motility in vitro [Lopez and Sheetz, 1993; Seitz et al., 2002], and their overexpression in neurons or non-neuronal cells interferes with kinesin mediated vesicle transport [Ebneth et al., 1998; Trinczek et al., 1999; Stamer et al., 2002; Mandelkow et al., 2004]. Although the inhibitory effects of the MAPs on kinesin mediated motility are well-documented, the mechanism of inhibition is not understood. Two possible modes of interference have been proposed: MAPs may inhibit binding by occupying part of the binding site such as the tubulin C-terminus [Ebneth et al., 1998; Trinczek et al., 1999], or MAP binding may interfere with the walking motility mechanism without affecting the binding sites of the kinesin motor domain [Lopez and Sheetz, 1993; Bulinski and Bossler, 1994]. Furthermore, all current studies have focused on the interference of MAPs with conventional kinesin. The effect of MAPs on other kinesins like Unc104, which play a large role in neuronal transport, is still an open question.

Here, we have used biochemical approaches to compare microtubule binding of dimeric constructs of *C. elegans* Unc104 (Unc104) and human conventional kinesin (kinesin) in the ADP state. We have focused on the motors in the ADP state because it is the initial state where weak interactions are first made with the microtubule surface. We show that ADP-Unc104 and ADP-kinesin bind microtubules with unique modes; Unc104 binds with 5-fold weaker affinity and 2-fold higher binding stoichiometry than kinesin. The interactions of ADP-Unc104 and ADP-kinesin with microtubules are largely mediated by positive charges in the K-loop and neck coiled-coil (respectively) as mutating these regions drastically reduced the binding affinity. By analyzing the binding of ADP-kinesin or ADP-Unc104 in the presence of MAP2c, we show that MAP2c acts as a competitive inhibitor of both ADP-Unc104 and ADP-kinesin with very similar K_Is. However, MAP2c seems to exhibit a moderate uncompetitive inhibition with ADP-kinesin, but not with ADP-Unc104. Taken together, Unc104 and kinesin in the ADP state bind microtubules with unique modes, both of which require positively charged elements that bind the tubulin C-termini.

EXPERIMENTAL PROCEDURES

Protein Expression and Purification

We used dimeric constructs of Unc104 (residues 1–446) and kinesin (residues 1–420) with GFP at the C-terminus. Kinesin, Unc104, and MAP2c were expressed and purified in *E. coli* as previously described [Pierce and Vale, 1998; Tomishige and Vale, 2000; Al-Bassam et al., 2002]. The K0 and 4-glu mutants were originally described [Thorn et al., 2000; Tomishige et al., 2002], and the proteins were purified as previously described.
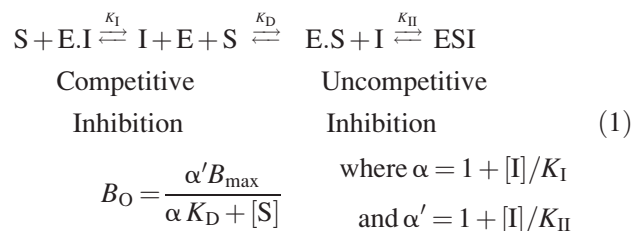
Microtubule Cosedimentation Assays

Microtubules were prepared from bovine tubulin (tubulin minus glycerol was purchased from Cytoskeleton Inc., Denver, CO) polymerized in 80 mM PIPES pH 6.8, 4 mM $MgCl_2$, 1 mM EGTA, 3 mM GTP and 50 μM taxol with incubation for 20 min at 34°C. For binding reactions, microtubules were mixed in a total of 50 μl

binding buffer (50 mM PIPES, pH 6.8, 4 mM MgCl$_2$, 1 mM EGTA, 1 mM DTT) at 4.1 μM polymerized tubulin dimer and varying concentrations of kinesin or Unc104 between 0.1 to 30 μM [Roger et al., 2004]. Multiple experiments were carried out to cover the full Unc104 or kinesin concentration range of binding to and beyond saturation. All these experiments contributed to the points shown in the curves. Prior to inhibition experiments, the MAP2c to microtubule saturation molar ratio was determined by microtubule cosedimatation without kinesin as previously described [Al-Bassam et al., 2002]. Competition reactions were carried out by incubating the motor with the microtubules for 30 min at room temperature, followed by the addition of MAP2c and incubation to steady state for 30 min afterwards. After centrifugation at 190,000g supernatants and pellets were separated, brought to equal volumes in SDS sample buffer and analyzed by SDS-PAGE. Coomassie stained gels were dried and analyzed by quantitative densitometry on a personal densitometer (Molecular Dynamics). The ratio of the MAP intensity to tubulin intensity was corrected for their respective molecular weights. The concentration of MAP, kinesin, and Unc104 were determined using protein assays and were compared with estimated values from the pellet and supernatant bands. The bound kinesin or Unc104 to polyermized tubulin ratio was plotted versus the free kinesin or Unc104 concentration and curves fitted to the experimental data using Prism software (GraphPad Co) using a single binding-site equation. Student's t-tests to evaluate the differences between binding parameters were performed in Prism using standard error values associated with the nonlinear regression.

Kinetic Inhibition Data Analysis

For inhibition analysis, Unc104 and kinesin were treated as substrates (S) and microtubules are treated as the enzyme (E), whereas MAP2c was treated as the inhibitor (I). Competitive and uncompetitive effects can be incorporated in the single binding site equation describing Unc104 or kinesin binding (B_O), as previously described [Segel, 1993] and shown below:

$$S + E.I \overset{K_I}{\rightleftharpoons} I + E + S \overset{K_D}{\rightleftharpoons} E.S + I \overset{K_{II}}{\rightleftharpoons} ESI$$

Competitive Inhibition   Uncompetitive Inhibition   (1)

$$B_O = \frac{\alpha' B_{max}}{\alpha K_D + [S]}$$

where $\alpha = 1 + [I]/K_I$

and $\alpha' = 1 + [I]/K_{II}$

K_D refers to the dissociation constant of motor binding, whereas B_{max} refers to the maximal bound motor/tubulin

stoichiometry. K_I and K_{II} are constants describing the competitive and uncompetitive inhibitory equilibria. A Lineweaver-Burk Plot can then be derived from the equation, then α and α' substituted for I and K_I or K_{II}:

$$\frac{1}{B_O} = \frac{1}{B_{max}} \left(1 + \frac{[I]}{K_I} \right) \left(\frac{(K_D)}{[B_{max}]} \frac{(1)}{[S]} \right) + \frac{1}{B_{max}} \left(\frac{1}{K_{II}} + [I] \right) \quad (2)$$

K_I can be determined by plotting different I concentrations versus the motor K_D/B_{max} values (Fig. 4), as follows:

$$\frac{K_D \text{ obs}^*}{B \text{ obs}^*} = \left(\frac{K_D}{B_{max}} \right) + [I] \left(\frac{K_D}{B_{max}} \frac{1}{K_{II}} \right), \quad \left(\frac{K_D}{B_{max}} \frac{1}{K_{II}} \right)$$

is the slope [I vs K_D/B_{max}] plot

$$K_I = K_D/(B_{max} * \text{slope})$$

* observed values in the different curve

K_{II} can be determined from different I concentrations versus $1/B_{max}$ (Fig. 5) as follows:

$$\frac{1}{B_{obs}^*} = \left(\frac{1}{B_{max}} \right) + [I] \left(\frac{1}{B_{max}} \frac{1}{K_{II}} \right), \left(\frac{1}{B_{max}} \frac{1}{K_{II}} \right)$$

is the slope [I vs K_D/B_{max}]plot

$$K_{II} = 1/(B_{max} * \text{slope})$$

RESULTS

Kinesin and Unc104 in the ADP State Bind Microtubules in Different Modes

Here, we examine the interactions of ADP-kinesin and ADP-unc104 with the microtubule, since it is the initial state in which these motors attach to the microtubule surface during their motility cycle. We first compared the microtubule binding (stoichiometry and affinity) of two dimeric constructs of kinesin and Unc104 in the ADP state using cosedimentation assays (see Materials and Methods). Wide concentration ranges of ADP-Unc104 or ADP-kinesin (0.1–30 μM) were incubated with a constant concentration of microtubules (4.1 μM polymerized tubulin dimer), and microtubule-bound motors were separated from soluble motors by ultracentrifugation (Fig. 1A). We used conditions (50 mM PIPES, 4 mM MgCl$_2$, 1 mM EGTA, pH 6.8) with relatively low ionic strength, in order to observe weak interactions of ADP-Unc104 or ADP-kinesin with microtubules. Lowering the ionic strength was shown to increase the attachment events to the microtubule surface [Vale et al., 1996]. At low motor concentrations (0.1–2 μM),
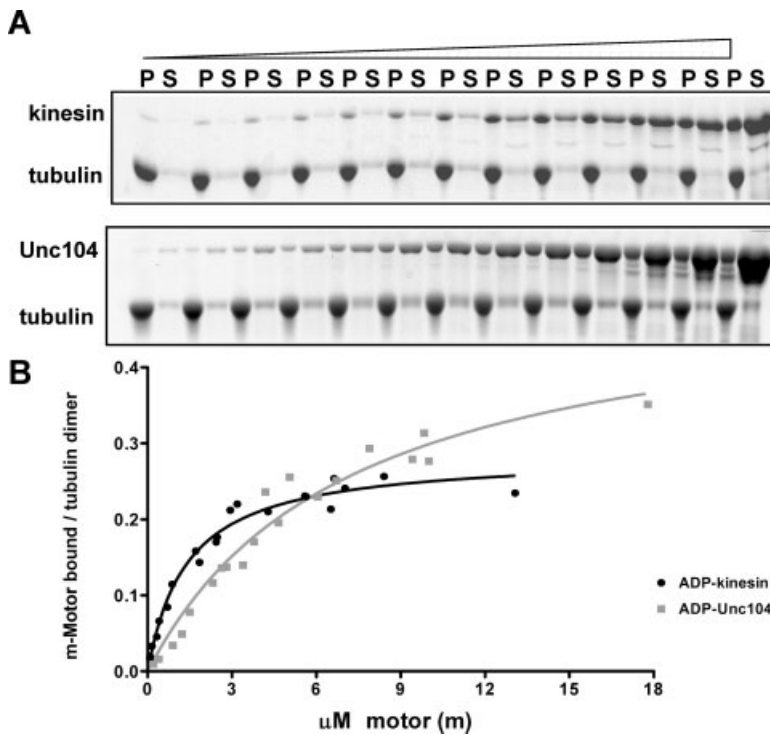
A

B

Fig. 1. ADP-Unc104 and ADP-kinesin binding to microtubules. (**A**) An example of microtubule cosedimentation with increasing amounts of kinesin (top) and Unc104 (bottom), in the presence of 4 mM ADP. These data represent experimental points used in curves in B. (**B**) ADP-kinesin (circles) and ADP-Unc104 (squares) microtubule binding curves; x-axis represents the total monomeric motor concentration (motor (m) in μM, while y-axis represents monomer motor bound per tubulin dimer ratio.

most of the kinesin is found in the pellet, bound to microtubules and absent from the supernatant (Fig. 1A, top panel), whereas Unc104, at similar concentrations, is distributed more equally in the supernatant and the pellet (Fig. 1A, lower panel). This suggests that ADP-Unc104 binds microtubules more weakly than ADP-kinesin. The ratio of Unc104 or kinesin bound in each cosedimeation experiment was plotted with respect to the total monomeric motor concentration in that experiment. The ADP-kinesin and ADP-Unc104 data fit well to a single binding site model. Analysis of the data using a single binding site model shows that ADP-kinesin binds microtubules with a 5-fold higher affinity than ADP-Unc104 (Fig. 1B). However, at saturation ADP-Unc104 binds microtubules with an approximately two fold higher stoichiometry compared to ADP-kinesin (Fig. 1B).

In order to interpret these binding stoichiometries, we considered that the kinesin neck forms a stable dimer, while Unc104 neck dimerization is a regulated activity that is likely to depend on the Unc104 concentration, occurring at or above 10 μM; above these concentrations, Unc104 dimerizes and undergoes processive motility [Tomishige et al., 2002]. Furthermore, we can assume that the binding site of each motor domain occupies a tubulin heterodimer on the microtubule wall. Taken together, our data suggest that on average an Unc104 dimer binds one tubulin heterodimer, whereas each kinesin dimer binds two tubulin heterodimers. This Unc104 binding stoichiometry confirms the conforma-

tion of Unc104 seen in a cryo-EM reconstruction of microtubules decorated with the same Unc104 construct in the ADP state. In these reconstructions, Unc104 shows a ''double-headed'' dimer bound to the microtubule. One motor domain is bound to the microtubule and the second motor domain is detached [Al-Bassam et al., 2003].

The weak affinity of ADP-Unc104 is surprising considering that the K-loop in Unc104 is believed to mediate additional motor interaction with the tubulin C-termini [Kikkawa et al., 2001; Al-Bassam et al., 2003]. Previous studies have shown that the K-loop of the Unc104 ortholog, KIF1A, binds the tubulin C-termini; this ionic interaction was abolished upon the cleavage of the C-termini by subtilisin [Okada and Hirokawa, 2000]. To understand the role of the K-loop in microtubule binding, we used an Unc104 construct in which the K-loop was replaced by the L12 sequence from conventional kinesin (termed K0), which was used in previous work [Tomishige et al., 2002]. We used co-sedimentation analysis to measure the binding affinity of the K0 mutant and compared it with Unc104 (Fig. 2A). We found that the K0 mutant binds microtubules with K_D of ~ 27 μM and 4-fold weaker affinity than wild-type Unc104 (Table I). In contrast, we found the affinity of the K0 mutant and wt Unc104 to microtubules was high in the presence of the non-hydrolyzable ATP analogue, AMPPNP (data not shown). The importance of the K-loop in maintaining the weak interaction of kinesin in the ADP state has been shown to be enhanced by the
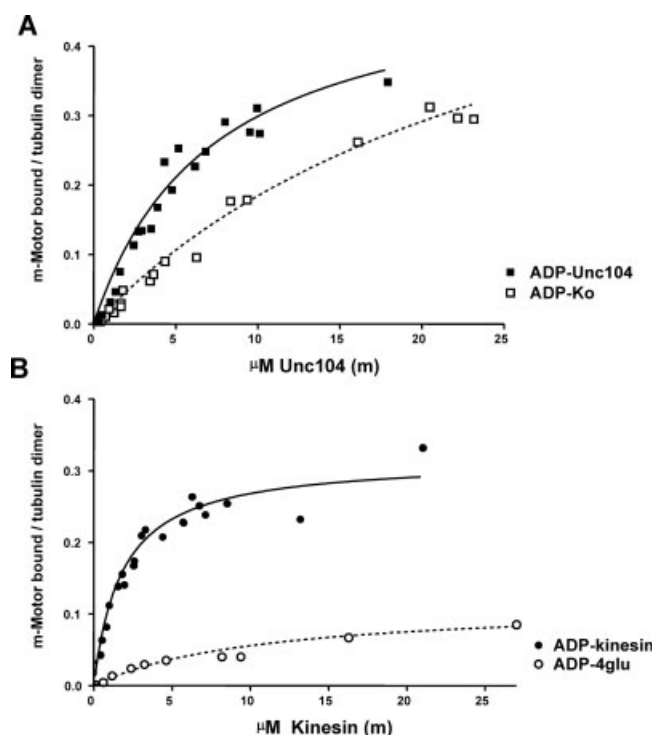
Fig. 2.   The Unc104 K-loop and kinesin neck play a major role in microtubule binding in the ADP state (**A**) Microtubule binding curve of ADP-K0 mutant (open squares) and wt ADP-Unc104 (full squares). Dissociation constants and binding stoichiometry, (listed in Table I), were determined by fitting the data to a single site binding model (see Materials and Methods). (**B**) Microtubule binding curve of ADP-4-glu mutant (open circles) and wt ADP-kinesin (full circles). Dissociation constants and stoichiometry were determined as in A.

TABLE I. Binding of ADP-kinesin, ADP-Unc104, and Mutants to Microtubules

| Motor | Stoichiometery (B_{max}) | | |
	K_D (µM)	m-mot-b/tub-d	mot-d/tub-d
ADP-Unc104-WT	7.15 ± 1.2	0.52 ± 0.05	~1:1
ADP-kinesin-WT	1.41 ± 0.16	0.29 ± 0.01	~1:2
ADP-Unc104 K0	27.1 ± 4.9	0.65 ± 0.10	~1.2:1
ADP-kinesin 4Glu	10.2 ± 3.6	0.12 ± 0.02	~1:4

K_D is the dissociation constants and B_{max} is the binding stoichiometry shown in two ways: monomer motor bound per tubulin dimer (m-mot-b/tub-d), or motor dimer per tubulin dimer (mot-d/tub-d).

stand whether the role of the positively charged residues in the kinesin neck is similar to that of the Unc104 K-loop in tethering the motor to the microtubule in the ADP state, we examined microtubule binding of a kinesin mutant in which these positively charged residues were mutated to glutamates (termed 4-Glu), a construct which was used in work by Thorn et al. [2000], and compared it to wt kinesin. Figure 2B shows that 4-Glu kinesin bound microtubules with a lower affinity (Table I) and decreased binding stoichiometry compared with wt kinesin (Table I). This result is distinct from the effect of neutralizing the K-loop in Unc104, which only affected the binding affinity and had little effect on binding stoichiometry. It is likely that the lysine to glutamate mutations may have caused a repulsive interaction with the acidic tubulin C-termini resulting in the dramatically lowered stoichiometry of the 4-Glu mutant.

addition of lysines in L-12 of KIF1D [Rogers et al., 2001]. The weakened binding affinity in the ADP state shows that K-loop-microtubule interaction plays a major role in its initial binding to the microtubule. The K-loop interaction with the tubulin C-termini suggests that the ADP-Unc104 is bound in a similar conformation, but the contribution of the motor domain to microtubule binding is minimal.

Although kinesin does not contain a K-loop, positively charged lysine residues that are moderately conserved in the first heptad of the coiled-coil neck are thought to be important for the weak microtubule interactions in the ADP state [Thorn et al., 2000]. Similar to the Unc104 K-loop, the kinesin neck lysines are thought to enhance the processive kinesin motility by binding the tubulin C-termini. The removal by subtilisin cleavage or removal of the positive charge in the neck caused defects in processive motility [Thorn et al., 2000]; Indeed, a recent electron microscopy study suggested that this neck region is likely to be attached to the microtubule between two bound kinesin motor domains, near the α-tubulin C-terminus [Skiniotis et al., 2003]. To under-

MAP2c Inhibits both Kinesin and Unc104 Binding to Microtubules in the ADP State

Thus far we have demonstrated that ADP-Unc104 and ADP-kinesin have unique microtubule binding modes that involve the K-loop and the neck coiled coil respectively. In the two motors, the presence of a positively charged region within or near the motor domain enhances their affinity to the microtubule by interacting with the tubulin C-termini. As the interaction of MAPs with microtubules is also mediated by the tubulin C-termini [Serrano et al., 1984, 1985], we next examined their effects on motor attachment in the ADP state. Specifically we wanted to see what effect MAP2c binding to microtubules would have on kinesin and Unc104 attachment in the ADP state. Since MAP2c binds the tubulin C-termini, this effect is comparable to removal of the positively charged regions (Unc104 K-loop and the kinesin neck) from the kinesins.

To explore the effects of MAP2c on motor-microtubule interactions, we carried out motor binding to microtubules in the presence of MAP2c. We treated Unc104 and kinesin as substrates and MAP2c as an in-
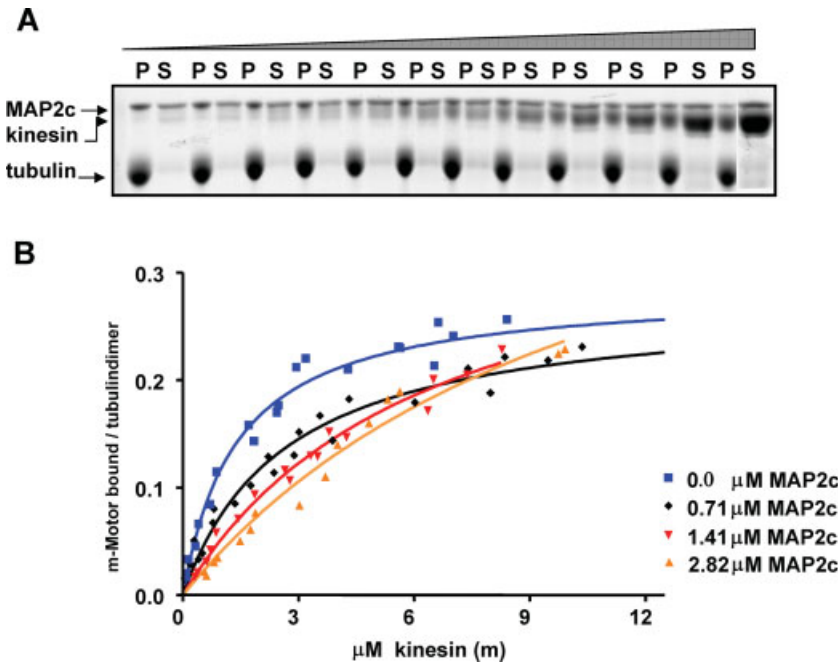
Fig. 3.   MAP2c inhibits ADP-kinesin binding to microtubules. Apparent dissociation constants (K_D) and binding stoichiometries (B_{max}) for each MAP2c concentration were obtained from fitted curves, and are shown in Table II. (**A**) Microtubule cosedimentation with increasing amounts of ADP-kinesin, in the presence of 2.82 µM MAP2c. Compared to Fig. 1A, there is more kinesin in the supernatant (S) and less in the pellet (P). These data are experimental points used for the saturated MAP2c curve in B (yellow triangles). (**B**) ADP-kinesin microtubule binding curves in the presence of varying concentrations of MAP2c. Data in the absence of inhibitor is shown in blue squares. Data in the presence of 0.71 µM, 1.41 µM, and 2.82 µM of MAP2c are shown in black diamonds, red triangles, yellow triangles, respectively.
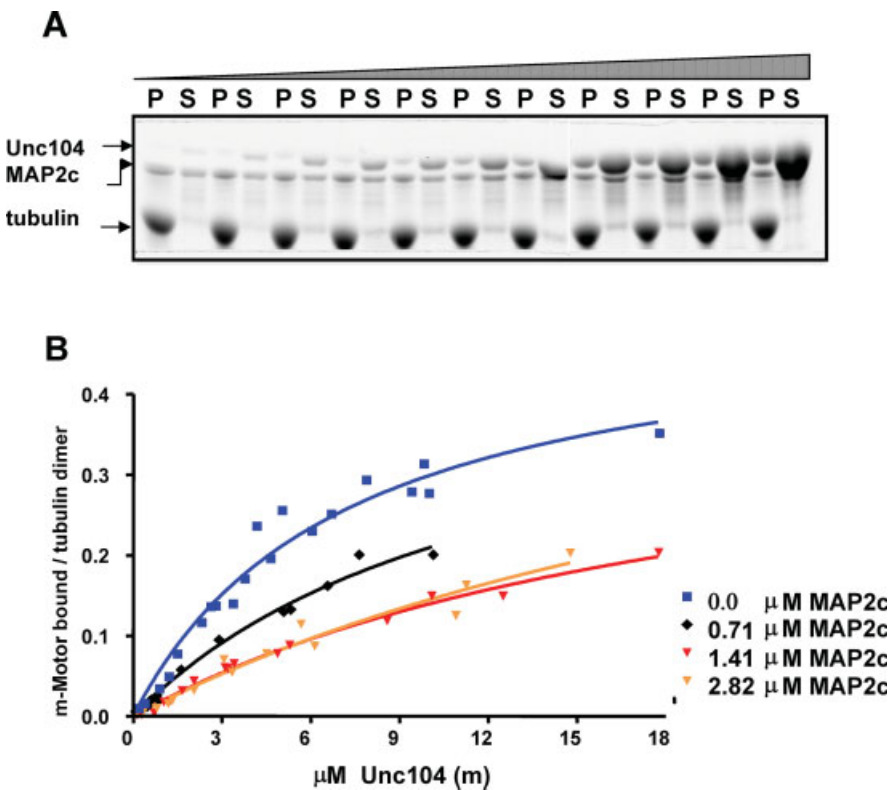

Fig. 4.   MAP2c inhibits ADP-Unc104 binding to microtubules. Apparent dissociation constants (K_D) and binding stoichiometries (B_{max}) for each MAP2c concentration were obtained from fitted curves, and are shown in Table II. (A). Microtubule cosedimentation with increasing amounts of ADP-Unc104, in the presence of 2.82 µM MAP2c. Compared to Fig. 2A, Unc104 is mostly in the supernatant (S) and little in the pellet (P). These data are experimental points used for the saturated MAP2c curve in B (yellow triangles). (B). ADP-Unc104 microtubule binding curves in the presence of varying concentrations of MAP2c.

hibitor (see Materials and Methods). We did not determine whether MAP2c (inhibitor) interacts directly with kinesin or Unc104 (substrates) in solution as such an interaction has never been reported and does not seem likely. We thus restricted our analysis to the inhibition effects that MAP2c exerts on the motors upon binding the microtubule. In brief, we added increasing concentrations of the motors (0.1–25 µM) to a fixed amount of microtubules (4.1 µM tubulin dimer), then directly added constant amounts of MAP2c and allowed the mixture to

reach steady state. The concentration range of MAP2c that is required to saturate microtubules was determined before the motor-competition experiments were performed, and three different concentrations (0.71, 1.41, and 2.82 μM) were chosen ranging from partial to full saturation. We observed (as we have previously shown) that MAP2c saturates microtubules at a ratio of 1 MAP2c to ~2.4 tubulin monomers or 1.2 tubulin dimer [Al-Bassam et al., 2002]. The soluble and microtubule bound components were separated by sedimentation then analyzed by SDS-PAGE and quantitated by staining and densitometry. Using this approach we generated ADP-motor binding curves in the presence of the three different MAP2c concentrations (0.71, 1.41, or 2.82 μM) that ranged from partial to full saturation of the MAP2c binding sites on microtubules.

　　　Saturation of microtubules with MAP2c (2.82 μM) clearly decreased the amount of kinesin binding to microtubules, but did not abolish it completely (Compare Figs. 1A top panel to Fig. 3A). Figure 4B shows microtubule binding curves for ADP-kinesin in the presence of three MAP2c concentrations compared to a binding curve in the absence of MAP2c. We observed that increasing the MAP2c concentration resulted in an increase in the apparent dissociation constant (K_D) of ADP-kinesin for microtubules, or a decrease in the apparent binding affinity for microtubules (Table II). We also observed an increase in the calculated stoichiometry of the microtubule bound kinesin.

　　　The ADP-Unc104 microtubule binding data in the presence of identical MAP2c concentrations (0.71, 1.41, and 2.82 μM) show that saturation of microtubules with MAP2c strongly inhibited Unc104 binding. MAP2c binding displaced most of the Unc104 off the microtubules (Fig. 4A). This severe effect is consistent with the weak affinity of ADP-Unc104 for microtubules (Table II). As for kinesin, we observed a decrease in microtubule binding affinity in the presence of MAP2c (Table II). We could not reach saturation of ADP-Unc104 binding in the presence of saturating MAP2c to microtubules (1.41 and 2.82 μM MAP2c). However, we did not observe any significant change in the stoichiometry calculated from the binding curves for ADP-Unc104 binding in the presence of different MAP2c concentrations. At the saturated MAP2c concentrations (2.82 μM), the increase in the Unc104 K_D was ~15 μM (Table II). This weakened ADP-Unc104 affinity in the presence of MAP2c is strikingly similar to the effects of removing positively charged residues in the Unc104 K-loop or the kinesin coiled-coil neck (Compare Figs. 2A to 3B, and 2B to 4B). Taken together the data suggest that MAP2c binding to microtubules inhibits ADP-Unc104 and ADP-kinesin attachment. This is reminiscent of the effect of removing positively charge lysine residues in the Unc104 K-loop and the kinesin neck.

TABLE II. ADP-kinesin and ADP-Unc104 Binding in the Presence of MAP2c

MAP2c (μM)	Stoichiometery (m-Mot-b/Tub-d)	Apparent K_D (μM)
A: ADP-kinesin binding		
0.0	0.29 ± 0.01	1.41 ± 0.16
0.71	0.29 ± 0.03	2.66 ± 0.31
1.41	0.39 ± 0.08	6.42 ± 0.90
2.82	0.53 ± 0.01	11.6 ± 2.7
B: ADP-Unc104 binding		
0.0	0.52 ± 0.05	7.15 ± 1.2
0.71	0.46 ± 0.11	11.9 ± 4.3
1.41	0.42 ± 0.04	19.5 ± 3.0
2.82	0.48 ± 0.18	22.9 ± 7.0

The apparent dissociation constants (K_D) and binding stoichiometries (m-Mot-b/Tub-d) are shown with respect to each MAP2c concentration.

Exploring Inhibition Mechanisms of MAP2c with Unc104 and Kinesin Binding

　　　In order to dissect the mechanisms for the inhibitory effects of MAP2c on ADP-kinesin and ADP-Unc104 binding to microtubules, we determined the relationship between the apparent K_D and binding stoichiometry at each MAP2c (inhibitor) concentration and the concentration of MAP2c itself. The two types of inhibition we explored were competitive and uncompetitive, classified in terms of the effect of inhibitor (MAP2c) on modifying either the apparent affinity (K_D) or binding stoichiometry (B_{max}) of substrate (ADP-kinesin or ADP-Unc104).

　　　In competitive inhibition, the inhibitor (MAP2c) competes for the binding site (in part or in full), decreasing the measured binding affinity of the kinesin or Unc104 (Fig. 5A). We used a relationship derived from a modified single binding site equation with modifiers that describe the effect of the competitor on the binding process for the substrate. This modified equation (Materials and Methods, Eq. 1) was used to determine if MAP2c exerts competitive inhibitory effects on either kinesin or Unc104. Typically there is a linear dependence of apparent K_D/B_{max} on the MAP2c concentration used (see Materials and Methods). We found that the change in the apparent K_D/B_{max} fits this type of linear dependence, suggesting that MAP2c competitively inhibits both ADP-Unc104 and ADP-kinesin binding to microtubules (Fig. 5B). The slope of these linear trends can be used to determine the equilibrium constant (K_I) describing the competitive inhibition (see Methods). Although the K_D and stoichiometry values of kinesin were different from those of Unc104, we obtain a strikingly similar K_I value for the effect of MAP2c on binding by either motor (Fig. 5C). Furthermore, the K_I of MAP2c for Unc104 and kinesin competitive inhibition are relatively close to the dissociation constant (K_D) of MAP2c binding to microtu-

A

Microtubule-MAP
(inhibited complex) $\underset{\text{Motor}}{\overset{K_I}{\rightleftarrows}}$ Microtubule + MAP + Motor $\underset{\text{MAP}}{\overset{K_D}{\rightleftarrows}}$ Microtubule-Motor
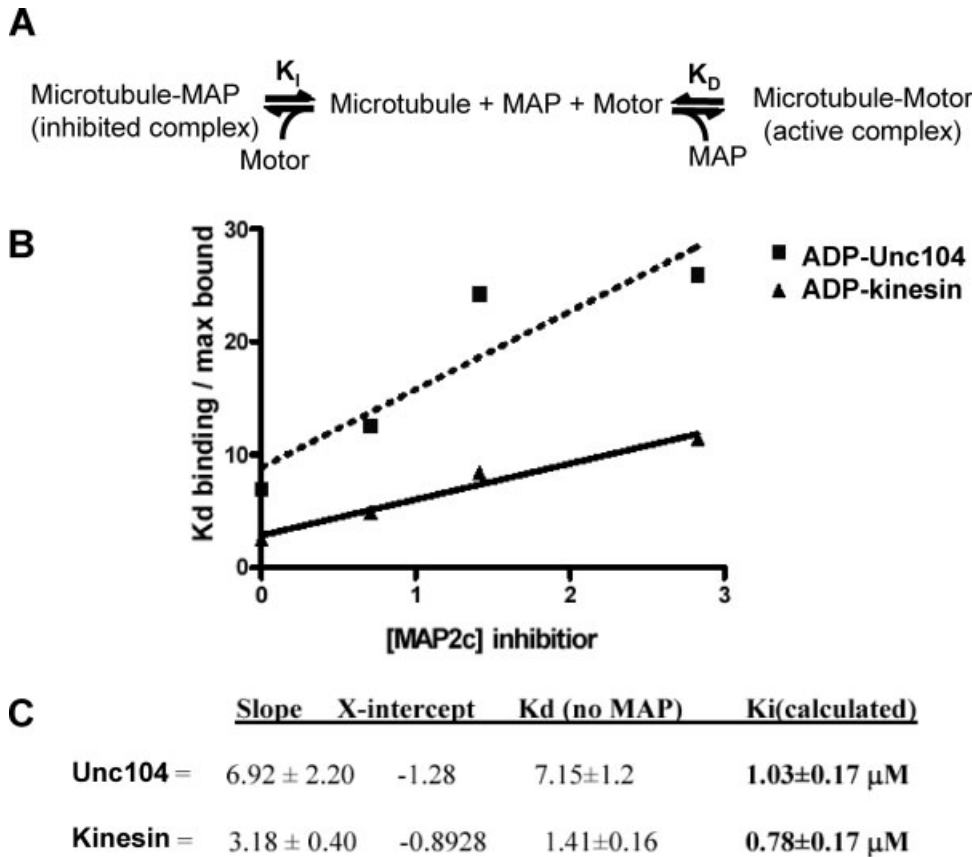(active complex)

B

■ ADP-Unc104
▲ ADP-kinesin

Fig. 5. MAP2c competitively inhibits both kinesin and Unc104 binding to microtubules in the ADP state: (**A**) Scheme for the motor-microtubule binding equilibrium, competed by MAP2c-microtubule binding equilibrium. K_I describes the competitive inhibition effect of MAP2c. (**B**). Plot describing the linear dependence of K_D for binding/maximal bound stoichiometry (K_D binding/B_{max}) on the MAP2c concentration (µM). In C, the slope and x intercept from the plot can be used to determine the K_I value (see Materials and Methods); K_I values for competitive inhibitory effects of MAP2c on ADP-Unc104 and ADP-kinesin are similar.

C

	Slope	X-intercept	Kd (no MAP)	Ki(calculated)
Unc104 =	6.92 ± 2.20	-1.28	7.15±1.2	**1.03±0.17 µM**
Kinesin =	3.18 ± 0.40	-0.8928	1.41±0.16	**0.78±0.17 µM**

bules previously measured (0.3–1 µM; see Coffey and Purich, 1995; Roger et al., 2004). These data are consistent with the idea that MAP2c binding to microtubules acts to compete with motor binding by occupying the sites for positively charged residues in the K-loop and the neck coiled coil binding on the tubulin C-termini.

We then asked if MAP2c mediates uncompetitive inhibitory effects on either ADP-kinesin or ADP-Unc104 binding to microtubules. Uncompetitive inhibition occurs when the inhibitor (MAP2c) decreases microtubule binding stoichiometry, rather than affinity (see Materials and Methods). In this type of inhibition, MAP2c would alter the modes of the motor microtubule interaction, independent of their effects on affinity (Fig. 6A). Using the modified single binding site equation (see Materials and Methods, Eq. 2), uncompetitive inhibition is characterized by linear dependence of $1/B_{max}$ of ADP-Unc104 or ADP-kinesin on the concentration of MAP2c. The slope of this linear relationship can be used to determine K_{II} (Fig. 6B). Using this approach, we found that MAP2c does not interfere with Unc104-microtubule interactions in an uncompetitive manner (since the slope of the plot is almost zero), whereas MAP2c exerts a moderate uncompetitive effect on kinesin-microtubule interaction (Fig. 6B). Thus, MAP2c may alter the binding of

ADP-kinesin to microtubules, favoring the single-head-bound state over the two-head-bound state, thus making the interaction similar to that of Unc104.

DISCUSSION

ADP-Unc104 and ADP-Kinesin Bind Microtubules with Unique Modes Mediated by the K-loop and the Neck Coiled Coil, Respectively

Our analysis shows that Unc104 and kinesin have different microtubule binding affinities and stoichiometries in the ADP state. The stoichiometries suggest that both motor domains of the ADP-kinesin dimer are likely to interact with the microtubule surface simultaneously. Only one motor domain of the ADP-Unc104 dimer attaches to the microtubules; the second motor domain is detached. This stoichiometry confirms what has been seen by electron microscopy and image analysis [Al-Bassam et al., 2003]. The unique dimerization modes of the Unc104 and kinesin neck domains may explain the difference in their microtubule binding stoichiometries. Unc104 neck dimerization is a regulated activity that may depend on the Unc104 concentration, occurring at or above 10 µM [Tomishige et al., 2002; Al-Bassam
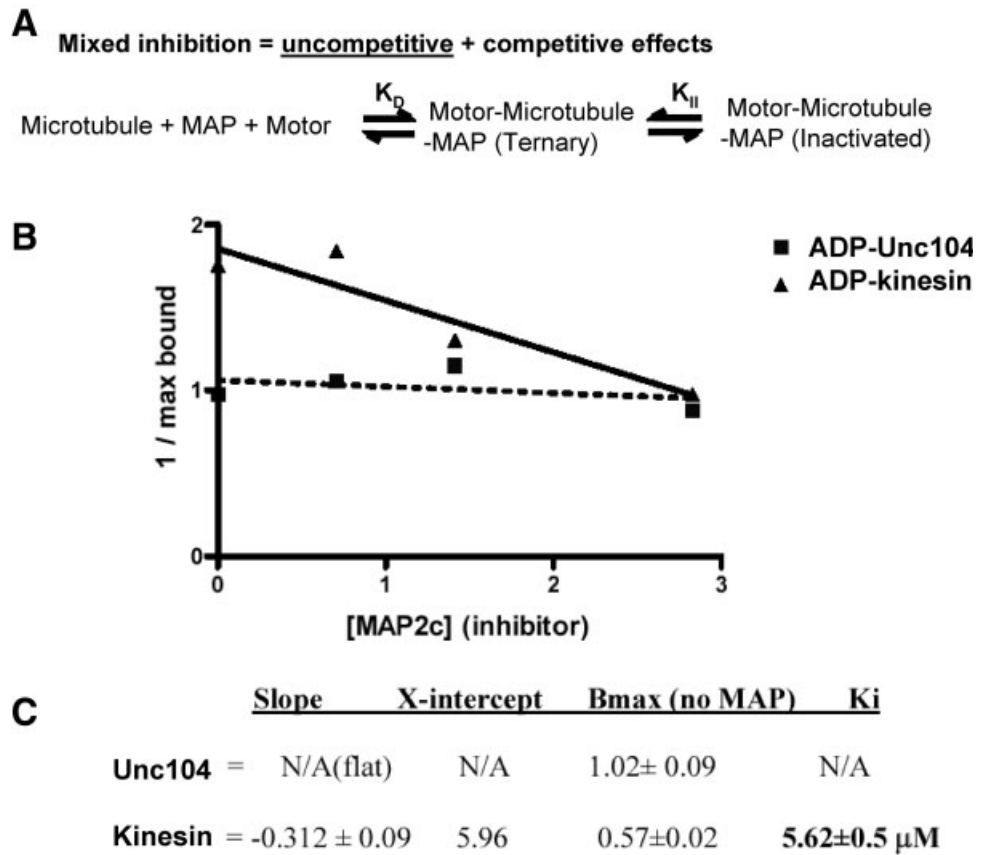
Fig. 6.   MAP2c mediates a moderate mixed inhibition for ADP-kinesin but not ADP-Unc104 binding (**A**). Scheme representing the motor-microtubule binding equilibrium for mixed inhibition. MAP2c binds the microtubule-motor complex forming a ternary complex, which causes a drop in binding activity, not its affinity; K_{II} describes the uncompetitive inhibition equilibrium of MAP2c. (**B**). Plot describing the linear dependence of the inverse of maximal bound on the MAP2c concentration (μM). (**C**). The slope and x intercept parameters from the plot can be used to determine the K_{II} value (see materials and methods). K_{II} values suggest that MAP2c only affects ADP-kinesin, not ADP-Unc104 binding to microtubules.

	Slope	X-intercept	Bmax (no MAP)	Ki
Unc104 =	N/A(flat)	N/A	1.02± 0.09	N/A
Kinesin =	-0.312 ± 0.09	5.96	0.57±0.02	**5.62±0.5 μM**

et al., 2003]. Thus, Unc104 dimerization occurs at concentrations similar to those required for microtubule binding (7 μM). This suggests that dimerization may be enhanced by the increase in the local concentration of ADP-Unc104 after microtubule binding at concentrations below 10 μM. Thus, Unc104 may first bind microtubules as a monomer and then dimerize. This is strikingly different from stably dimeric kinesin, where both motor domains are able to interact with the microtubule as a consequence of a single collision event, resulting in the observed binding stoichiometry. We believe that the state in which both the ADP-kinesin motor domains are bound to the microtubule is forced by the absence of ATP in our experiment and would likely be extremely short lived in vivo.

The removal of positively charged residues in the Unc104 K-loop (K0) and kinesin neck coiled-coil (4-Glu) suggests that the motors' unique modes of binding to microtubules in the ADP state are primarily mediated by these elements. These elements interact directly with the tubulin C-termini whose removal by subtlisin inhibits binding [Okada and Hirokawa, 2000; Thron et al., 2000]. The four-fold drop in ADP-Unc104 affinity brought about by the removal of the K-loop suggests that its positive charges mediate a considerable fraction of the ADP-

Unc104 binding affinity. The removal of the positive charge in the kinesin neck coiled-coil (the 4-Glu kinesin mutant) induced a three-fold drop in the kinesin binding stoichiometry and seven-fold drop in binding affinity. Even though the motor domains are positioned at the microtubule interface, the affinity is very weak and the motor domains are anchored by their positively charged regions to the tubulin C-termini. Both the Unc104 K-loop and the kinesin neck seem to only influence the binding affinity; the kinesin neck may promote the double-bound state on the microtubules.

We have previously shown that the microtubule-bound ADP-Unc104 and AMPPNP-Unc104 states differ by a 5° rotation of the motor domain [Al-Bassam et al., 2003]. This rotation is not observed in conventional kinesin [Rice et al., 1999]. We suggested this nucleotide dependent rotation may reflect an Unc104 weak binding state distinct from that of conventional kinesin [Al-Bassam et al., 2003]. The weakened ADP-Unc104 affinity is biologically relevant for its unique motility function. Upon dimerization at high concentrations, Unc104 undergoes processive, hand-over-hand motility along microtubules that is two to three times faster than kinesin [Tomishige et al., 2002]. Our data on the weak interactions of ADP-Unc104 and kinesin to microtubules sheds
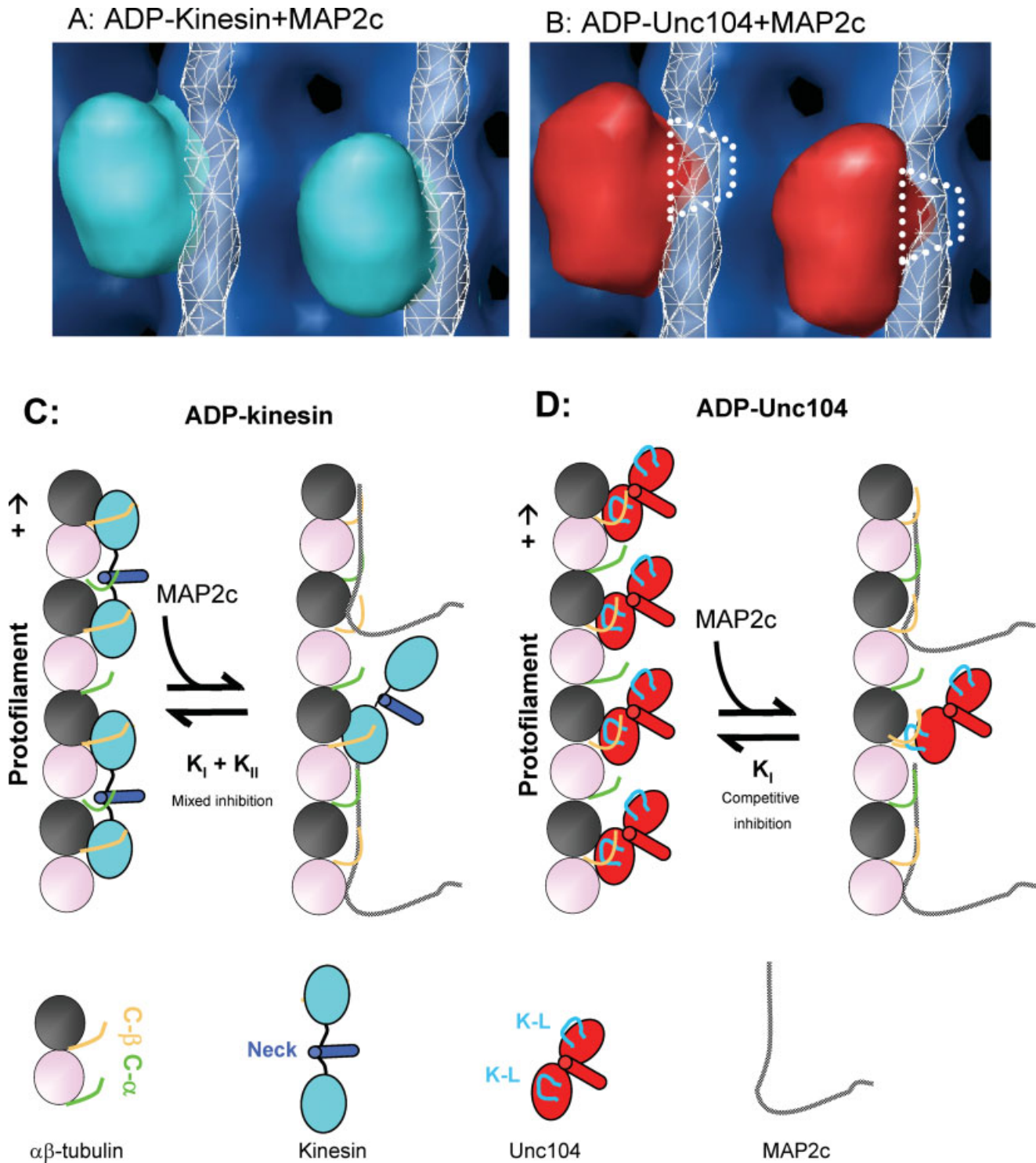
Fig. 7. ADP-kinesin and ADP-Unc104 binding to microtubules and its modulation by MAP2c. (**A,B**) 3D maps of the kinesin (blue) and Unc104 (red) motor domains bound to microtubules. Microtubule-bound MAP2c is shown in wire frame representation. In B, the Unc104 K-loop and MAP2c densites overlap, suggesting that they might compete for the C-terminus of β-tubulin. These 3D-maps were adapted from Rice et al., (1999), Al-Bassam et al. (2002) and Al-Bassam et al. (2003). Microtubules are shown with their plus ends pointed to the top of the page. (**C**) Our data suggest that both motor domains of ADP-kinesin bind to microtubules. Interactions between the C-terminus of α-tubulin (green) and a positively charged region of the coiled coil neck (blue) contribute to the apparent affinity (left panel). MAP2c competes for the C-terminus resulting in weak binding by only one of the motor domains of the dimer (right panel). (**D**) Interactions between the Unc104 K-loop (blue, K–L) and the C-terminus of β-tubulin (yellow) contribute to the ADP-Unc104—microtubule apparent affinity (left panel). MAP2c competes for the C-terminus, lowering the affinity (right panel).

light on the initial attachment of these motors and, more importantly, on their weakly bound state during the hand-over-hand motility process (after ATP hydrolysis and phosphate release). In hand-over-hand motility, the association and dissociation of the motor domain are the rate limiting steps in motility, both of which are dependent on weak interactions in the ADP state. The Unc104 K-loop and the kinesin neck coiled-coil may be responsible for maintaining these weak interactions during the motility cycle. However, the weak affinity of ADP-Unc104 compared to ADP-kinesin would be consistent with its fast release compared to the kinesin motor domain, as previously suggested [Tomishige et al., 2002]. Furthermore, the role of the K-loop would be to support processivity of dimeric Unc104 by preventing its dissociation from the microtubule while its motor domain is weakly bound to the microtubule surface, similar to what has been suggested for the kinesin neck coiled-coil [Thorn et al., 2000; Tomishige et al., 2002]. Based on the Unc104 and kinesin conformations in Cryo-EM, We expect the Unc104 K-loop to bind the β-tubulin C-terminus, which is adjacent to the motor binding site (Fig. 7C), whereas the kinesin neck coiled-coil likely binds the α-tubulin C-terminus, which is located between two adjacent motor binding sites (Fig. 7D). This may explain the different defects we observed for mutants in which the K-loop and neck coiled-coil were mutated. The defects observed with the mutants correlate well with the competitive modes of MAP2c-mediated inhibition seen for kinesin and Unc104, since MAP2c likely binds both α and β tubulin C-termini (Fig. 7C, D).

The inhibitory Effects of MAP2c on Unc104 and Kinesin Binding to Microtubules

Using steady state kinetics, we show that MAP2c behaves like a classic competitive inhibitor of ADP-Unc104 and ADP-kinesin binding to microtubules; the K_Is of MAP2c competitive inhibition for kinesin and Unc104 are very similar even though ADP-Unc104 and kinesin binding modes to microtubules are different. The K_I values are almost identical to the microtubule binding affinity measured [Coffey and Purich, 1995], indicating that the MAP2c binding site overlaps that of kinesin and Unc104. It seems likely that MAP binding to the tubulin C-termini prevents the Unc104 K-loop and the kinesin neck coiled-coil from interacting with them (Figs. 7C and 7D). Comparisons of the MAP2c, kinesin and Unc104 decorated microtubule maps support these observations. The elongated MAP2c binding site is very close to the kinesin motor binding interface on the protofilament ridges (Figs. 7A and 7B) and overlaps with the Unc104 K-loop density bound to the β-tubulin C-termini (Fig. 7B; Al-Bassam et al., 2002, 2003). These comparisons support the idea that the microtubule-bound

MAP2c, which extends over both α and β tubulin C-termini, uniquely interferes with the distinct modes of ADP-Unc104 and ADP-kinesin binding to microtubules. However, another possible explanation for the observed effects is that other regions within the MAP2c repeat domain interfere with ADP-Unc104 and kinesin binding by occupying part of the motor binding site (Fig. 7).

Biological Implications of MAP2c Interference with Kinesin and Unc104 Motility

MAPs such as MAP2 and tau stabilize microtubules by reducing dynamic instability, promote the assembly of microtubules into parallel bundles, and perform other functions in cytoskeletal organization [Cassimeris and Spittle, 2001; Dehmelt and Halpain, 2005]. Furthermore, the relatively high concentration of these MAPs inside neuronal axons and dendrites makes our data directly relevant to the cellular environment [Dehmelt and Halpain, 2005]. These MAPs also inhibit microtubule motor-driven cargo transport both in vitro and in vivo [Bulinski et al., 1997; Ebneth et al., 1998; Seitz et al., 2002; Stamer et al., 2002; Mandelkow et al., 2004]. Overexpression of tau in CHO and N2a cells impaired the anterograde transport of mitochondria, endoplasmic reticulum, and other organelles [Ebneth et al., 1998]. This effect was due to inhibition of their attachment to the microtubule track, rather than reduction of movement velocity [Trinczek et al., 1999]. Interestingly, plus-end directed organelle movements were more strongly impaired by tau than minus-end directed movements, suggesting that kinesin-mediated motility may be preferentially inhibited over dynein-dependent motility [Trinczek et al., 1999]. The proposed mechanism for inhibition of organelle transport is supported by in vitro studies of single kinesin molecules moving along microtubules. Both MAP2c and tau were shown to interfere with kinesin's motility by inhibiting its microtubule attachment [Seitz et al., 2002]. Our results demonstrating competitive and uncompetitive inhibition of motor binding by MAP2c are consistent with these conclusions and suggest that the tubulin C-termini are critical for productive interaction of ADP-containing kinesin motors with microtubules. Although we propose that inhibition is mediated by the microtubule binding domain of MAP2c competing for the C-termini, there is evidence to suggest that the projection domains of MAP2 (at least for its longer isoforms MAP2a/b) may also contribute to the inhibition of motor-driven transport [Lopez and Sheetz, 1993].

Although the competitive inhibition of ADP-Unc104 and ADP-kinesin binding to microtubules by MAP2c in vitro is consistent with observations made in MAP overexpressing neurons as well as other cell types in culture [Ebneth et al., 1998; Stamer et al., 2002], it

does not explain why there is no inhibition of kinesin-driven transport by endogenous levels of MAPs in vivo. One possible explanation is that the inhibition we have demonstrated is modulated by the dynamics of MAP-microtubule interactions. The dynamics of MAP association and dissociation are influenced by multiple factors, including phosphorylation by protein kinases that target specific residues within the microtubule binding repeats [Ebneth et al., 1998; Ozer and Halpain, 2000]. Phosphorylation of KXGS sites decreases the affinity of MAPs for microtubules [Illenberger et al., 1996; Ozer and Halpain, 2000], allowing kinesin to attach and move along microtubules. Such phosphorylation might enable kinesin-dependent transport to take place in a locally-regulated fashion, and thereby orchestrate the control of intracellular trafficking and the development of neurites.

ACKNOWLEDGMENTS

REFERENCES

Al-Bassam J, Ozer RS, Safer D, Halpain S, Milligan RA. 2002. MAP2 and tau bind longitudinally along the outer ridges of microtubule protofilaments. J Cell Biol 157:1187–1184.

Al-Bassam J, Cui Y, Klopfenstein D, Carragher BO, Vale RD, Milligan RA. 2003. Distinct conformations of the kinesin Unc104 neck regulate a monomer to dimer motor transition. J Cell Biol 163:743–744.

Brown A. 2003. Axonal transport of membranous and nonmembranous cargoes: a unified perspective. J Cell Biol 160:817–814.

Bulinski JC, Bossler A. 1994. Purification and characterization of ensconsin, a novel microtubule stabilizing protein. J Cell Sci 107:2839–2844.

Bulinski JC, McGraw TE, Gruber D, Nguyen HL, Sheetz MP. 1997. Overexpression of MAP4 inhibits organelle motility and trafficking in vivo. J Cell Sci 110:3055–3064.

Cassimeris L, Spittle C. 2001. Regulation of microtubule-associated proteins. Int Rev Cytol 210:163–226.

Coffey RL, Purich DL. 1995. Non-cooperative binding of the MAP-2 microtubule-binding region to microtubules. J Biol Chem 270:1035–1044.

Dehmelt L, Halpain S. 2004. Actin and microtubules in neurite initiation: are MAPs the missing link? J Neurobiol 58:18–33.

Dehmelt L, Halpain S. 2005. The MAP2/Tau family of microtubule-associated proteins. Genome Biol 6:204.

Desai A, Mitchison TJ. 1997. Microtubule polymerization dynamics. Annu Rev Cell Dev Biol 13:83–84.

Ebneth A, Godemann R, Stamer K, Illenberger S, Trinczek B, Mandelkow E. 1998. Overexpression of tau protein inhibits kinesin-dependent trafficking of vesicles, mitochondria, and endoplasmic reticulum: implications for Alzheimer's disease. J Cell Biol 143:777–794.

Gamblin TC, Nachmanoff K, Halpain S, Williams RC, Jr. 1996. Recombinant microtubule-associated protein 2c reduces the dynamic instability of individual microtubules. Biochemistry 35:12576–12584.

Goldstein LS. 2001. Molecular motors: from one motor many tails to one motor many tales. Trends Cell Biol 11:477–484.

Gordon-Weeks PR. Microtubules and growth cone function. 2004. J Neurobiol 58:70–74.

Hall DH, Hedgecock EM. 1991. Kinesin-related gene Unc-104 is required for axonal transport of synaptic vesicles in C. elegans. Cell 65:837–844.

Hirokawa N, Takemura R. 2005. Molecular motors and mechanisms of directional transport in neurons. Nat Rev Neurosci 6:201–204.

Hoenger A, Sack S, Thormahlen M, Marx A, Muller J, Gross H, Mandelkow E. 1998. Image reconstructions of microtubules decorated with monomeric and dimeric kinesins: comparison with x-ray structure and implications for motility. J Cell Biol 141:419–424.

Illenberger S, Drewes G, Trinczek B, Biernat J, Meyer HE, Olmsted JB, Mandelkow EM, Mandelkow E. 1996. Phosphorylation of microtubule-associated proteins MAP2 and MAP4 by the protein kinase p110mark. Phosphorylation sites and regulation of microtubule dynamics. J Biol Chem 271:834–844.

Kikkawa M, Okada Y, Hirokawa N. 2000. 15 A resolution model of the monomeric kinesin motor, KIF1A. Cell 100:241–252.

Kikkawa M, Sablin EP, Okada Y, Yajima H, Fletterick RJ, Hirokawa N. 2001. Switch-based mechanism of kinesin motors. Nature 411:439–444.

Kowalski RJ, Williams RC, Jr. 1993. Microtubule-associated protein 2 alters the dynamic properties of microtubule assembly and disassembly. J Biol Chem 268:9847–9855.

Lopez LA, Sheetz MP. 1993. Steric inhibition of cytoplasmic dynein and kinesin motility by MAP2. Cell Motil Cytoskeleton 24:1–4.

Mandelkow EM, Thies E, Trinczek B, Biernat J, Mandelkow E. 2004. MARK/PAR1 kinase is a regulator of microtubule-dependent transport in axons. J Cell Biol 167:99–94.

Mitchison T, Kirschner M. 1984. Dynamic instability of microtubule growth. Nature 312:237–242.

Nangaku M, Sato-Yoshitake R, Okada Y, Noda R, Takemura , Yamazaki H, Hirokawa N. 1994. KIF1B, a novel microtubule plus end-directed monomeric motor protein for transport of mitochondria. Cell 79:1209–1214.

Ozer RS, Halpain S. 2000. Phosphorylation-dependent localization of microtubule-associated protein MAP2c to the actin cytoskeleton. Mol Biol Cell 11:3573–3574.

Okada Y, Hirokawa N. 2000. Mechanism of the single-headed processivity: diffusional anchoring between the K-loop of kinesin and the C terminus of tubulin. Proc Natl Acad Sci 97:640–644.

Pierce DW, Vale RD. 1998. Assaying processive movement of kinesin by fluorescence microscopy. Methods Enzymol 298:154–164.

Pierce DW, Hom-Booher N, Otsuka AJ, Vale RD. 1999. Single-molecule behavior of monomeric and heteromeric kinesins. Biochemistry 38:5412–5414.

Rice S, Lin AW, Safer D, Hart CL, Naber N, Carragher BO, Cain SM, Pechatnikova E, Wilson-Kubalek EM, Whittaker M, Pate E, Cooke R, Taylor EW, Milligan RA, Vale RD. 1999. A structural change in the kinesin motor protein that drives motility. Nature 402:778–784.

Roger B, Al-Bassam J, Dehmelt L, Milligan RA, Halpain S. 2004. MAP2c, but not tau, binds and bundles F-actin via its microtubule binding domain. Curr Biol 14:363–364.

Rogers KR, Weiss S, Crevel I, Brophy PJ, Geeves M, Cross R. 2001. KIF1D is a fast non-processive kinesin that demonstrates novel K-loop-dependent mechanochemistry. EMBO J 20:5101–5113.

Romberg L, Pierce DW, Vale RD. 1998. Role of the kinesin neck region in processive microtubule-based motility. J Cell Biol 140:1407–1416.

Segel IH. 1993. Enzyme Kinetics: Behavior and Analysis of Rapid Equilibrium and Steady State Enyzme Systems. New York: Wiley. pp 18–159.

Seitz A, Kojima H, Oiwa K, Mandelkow EM, Song YH, Mandelkow E. 2002. Single-molecule investigation of the interference between kinesin, tau and MAP2c. EMBO J 21:4896–4894.

Serrano L, Avila J, Maccioni RB. 1984. Controlled proteolysis of tubulin by subtilisin: localization of the site for MAP2 interaction. Biochemistry 23:4675–4684.

Serrano L, Montejo de Garcini E, Hernandez MA, Avila J. 1985. Localization of the tubulin binding site for tau protein. Eur J Biochem 153:595–604.

Setou M, Seog DH, Tanaka Y, Kanai Y, Takei Y, Kawagishi M, Hirokawa N, 2002. Glutamate-receptor-interacting protein GRIP1 directly steers kinesin to dendrites. Nature 417:83–87.

Skiniotis G, Surrey T, Altmann S, Gross H, Song YH, Mandelkow E, Hoenger A. 2003. Nucleotide-induced conformations in the neck region of dimeric kinesin. EMBO J 22:1518–1524.

Stamer K, Vogel R, Thies E, Mandelkow E, Mandelkow EM. 2002. Tau blocks traffic of organelles, neurofilaments, and APP vesicles in neurons and enhances oxidative stress. J Cell Biol 156:1051–1063.

Thorn KS, Ubersax JA, Vale RD. 2000. Engineering the processive run length of the kinesin motor. J Cell Biol 151:1093–1094.

Tomishige M, Vale RD. 2000. Controlling kinesin by reversible disulfide cross-linking. Identifying the motility-producing conformational change. J Cell Biol 151:1081–1092.

Tomishige M, Klopfenstein DR, Vale RD. 2002. Conversion of Unc104/KIF1A kinesin into a processive motor after dimerization. Science 297:2263–2264.

Trinczek B, Ebneth A, Mandelkow EM, Mandelkow E. 1999. Tau regulates the attachment/detachment but not the speed of motors in microtubule-dependent transport of single vesicles and organelles. J Cell Sci 112:2355–2364.

Vale RD, Funatsu T, Pierce DW, Romberg L, Harada Y, Yanagida T. 1996. Direct observation of single kinesin molecules moving along microtubules. Nature 380:451–453.

Vale RD, Milligan RA. 2000. The way things move: Looking under the hood of molecular motor proteins. Science 288:88–94.

Zhou HM, Brust-Mascher I, Scholey JM. 2001. Direct visualization of the movement of the monomeric axonal transport motor UNC-104 along neuronal processes in living *Caenorhabditis elegans*. J Neurosci 21:3749–3754.